

original training data are representative of the underlying distribution, then this test shows quite excellent performance. The graphic display for the results shown in Fig. 5 represents a three-layer network. The size of the rectangular symbols represents the magnitude of the value of each node. The size of output layer symbol 20 in Fig. 5a indicates that this result is a rotating stall condition. The results of a normal run for Rotor-A and Rotor-C are shown by the size of symbols 21 and 22 in Fig. 5b and 5c, respectively.

A monitoring expert system has been designed to assist the operators to monitor the compressors. The expert system consists of three major subsystems: knowledge-based diagnostic subsystem; neural network subsystem; and graphical user interface. The prototype system has been initiated for a complete compressor monitoring system in which several software packages are integrated.

### Conclusions

The feasibility of neural networks to detect the compressor stall has been demonstrated. The selection of features from the blade strain gage data is critical to the successful detection of rotating stall and normal run. The integration of neural network and expert system is a powerful tool for compressor stall monitoring.

### Acknowledgments

This work was supported by AEDC/AF and NASA/Ames Research Center under Grant NAG2-596 and by the University of Tennessee—Calspan Center for Space Transportation and Applied Research under NASA Grant NAGW-1195. The authors thank Carlos Tirres and U. G. Nordstrom of AEDC for their guidance. Frank W. Steinle of NASA Ames was the technical monitor.

### References

<sup>1</sup>Garnier, V. H., Epstein, A. H., and Greitzer, E. M., "Rotating Waves as a Stall Inception Indication in Axial Compressor," American Society of Mechanical Engineers Paper 90-GT-156, June 1990.

<sup>2</sup>Rumelhart, D. E., Hinton, G. E., and Williams, R. J., "Learning Internal Representations by Error Propagation," *Parallel Distributed Processing*, edited by D. E. Rumelhart and J. L. McClelland, Vol. I, MIT Press, Cambridge, MA, 1987, pp. 318–362.

asymmetry and sideforce magnitude. The objective of the present water tunnel study is to provide information that may lead to a better understanding of the effect of the nose-boom on forebody vortex flow. Four different models were used to study in detail the interaction between the forebody vortex flow and the nose-boom wake flow. Specifically, the study would try to establish conditions under which the nose-boom would increase or decrease the zero-sideslip asymmetric sideforce.

### II. Experimental Setup

The experiment was conducted in the Eidetics 2436 Flow Visualization Water Tunnel.<sup>5</sup> Two forms of visualization were performed 1) off-surface dye visualization; and 2) surface dye-visualization. Details of the techniques are described in Ref. 5. Three F-16 models were used: a 1/20th-scale full model (model 1; total length = 75.81 cm, including a 3.29-cm nose-boom); the 1/10th-scale forebody section model (model 2; total length = 84.14 cm, including a 5.72-cm nose-boom); and a 3/10th-scale nose-tip model (model 3; total length = 57.86 cm, including a 19.76-cm nose-boom). Models 1 and 2 were tested with and without the standard nose-boom. The primary advantage of using three different models is that the scale of each one can be tailored for specific purposes. In particular, the full model was for visualization of the overall flow and interaction between vortices and various parts of the aircraft configuration. The forebody-section model was used for detailed visualization of the forebody vortices. The nose-tip model was for detailed visualization of the flow at the nose-tip region. One drawback of using different models, however, was that results of the three models would not be identical due to the sensitivity of the forebody flow to even minute physical differences between the models. The difference in Reynolds number introduced further dissimilarities. To a certain degree, this may restrict direct comparisons of the results. Additional tests were performed on a 6% scale F/A-18 forebody section model (model 4; length = 60.2 cm without the nose-boom) with a 3.61-cm-long and 0.32-cm-diam cylindrical nose-boom. The baseline model without the nose-boom had been studied extensively.<sup>5</sup>

Tests for the F-16 models were conducted for angles of attack from 15–60 deg, mostly at  $\beta = 0$  deg and in 5-deg increments. For the F/A-18 model, tests were conducted for angle of attack from 15–65 deg, again in 5-deg increments. The tests were conducted at flow speeds from 5.1–10.2 cm/s, corresponding to a Reynolds number range of about  $0.47 \times 10^3$  to  $0.94 \times 10^3$  per cm. The low-test Reynolds number ensured the flow to be laminar before separation.

### III. Results and Discussions

Results of the F-16 models 1 and 2 show that the nose-boom strongly affects the forebody vortex asymmetry. Without the nose-boom, the forebody flows over both models remain visually symmetric from  $\alpha = 15$  to 60 deg. The effect of the nose-boom is strongly dependent on the angle of attack. The forebody vortex flow for model 1 with the nose boom becomes visibly asymmetric for  $\alpha$ 's above  $\sim 45$  deg. The orientation of the forebody vortices and the degree of asymmetry is dependent on the angle of attack. The vortices can switch between "left-vortex-high" and "right-vortex-high" orientations through the angle of attack range. Initially, the degree of asymmetry increases with the angle of attack. Further increasing the angle of attack, however, eventually leads to a reduction in the vortex asymmetry. Above  $\alpha = 60$  deg the forebody vortices become essentially symmetric, at least in a time-average sense.

Details of the forebody flow are more readily revealed by results of the forebody-section model (model 2). The flows over models 1 and 2 are similar. For model 2, the forebody vortex asymmetry was observed to begin at  $\alpha$  above about 45 deg, reach a maximum at approximately 55 deg, and then reduce significantly when  $\alpha$  increases to 60 deg. At higher

## Effect of a Nose-Boom on Forebody Vortex Flow

T. Terry Ng\*

University of Toledo, Toledo, Ohio 43606

### I. Introduction

At high angles of attack, the sensitivity of the leeward vortices of a slender forebody to external disturbances is well documented. One source of such disturbances on many existing aircraft configurations is the nose-boom. Studies have shown that the wake of a nose-boom can influence substantially the overall forebody flow. There are, however, conflicting reports of increases (e.g., Refs. 1 and 2) and reductions (e.g., Refs. 3 and 4) of the zero-sideslip forebody vortex

Received June 8, 1991; revision received Sept. 13, 1991; accepted for publication Sept. 13, 1991. Copyright © 1991 by the American Institute of Aeronautics and Astronautics, Inc. All rights reserved.

\*Associate Professor, Department of Mechanical Engineering, Member AIAA.

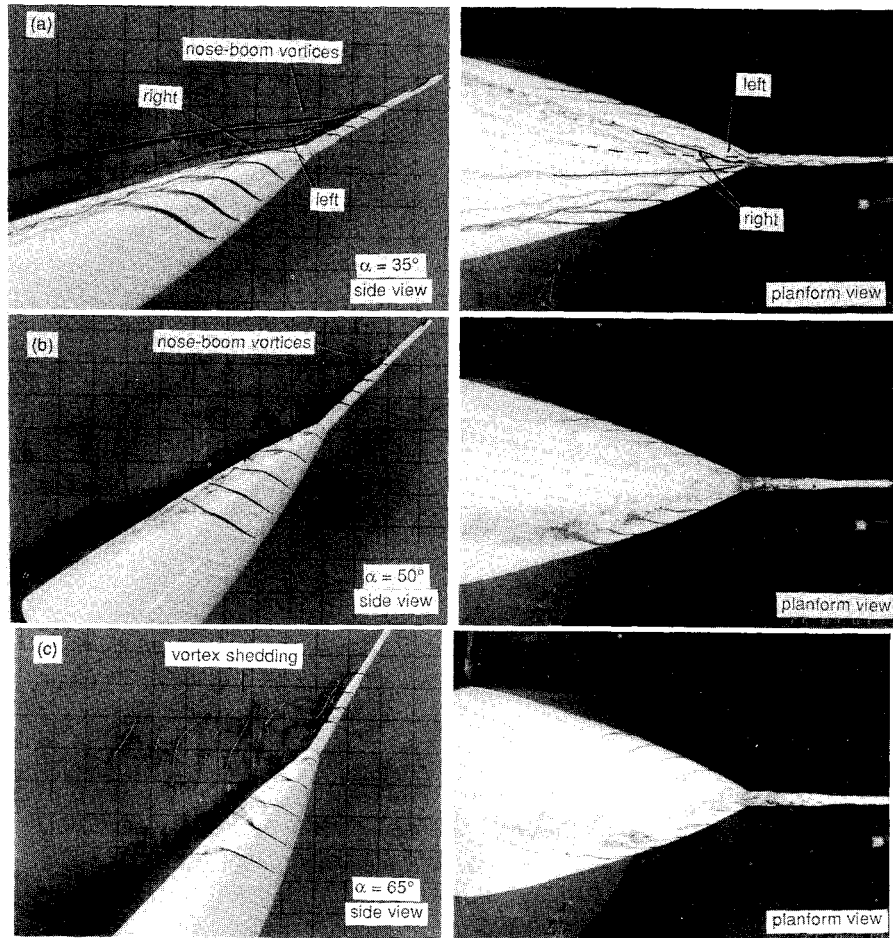


Fig. 1 Flows over the F-16 nose-tip model.

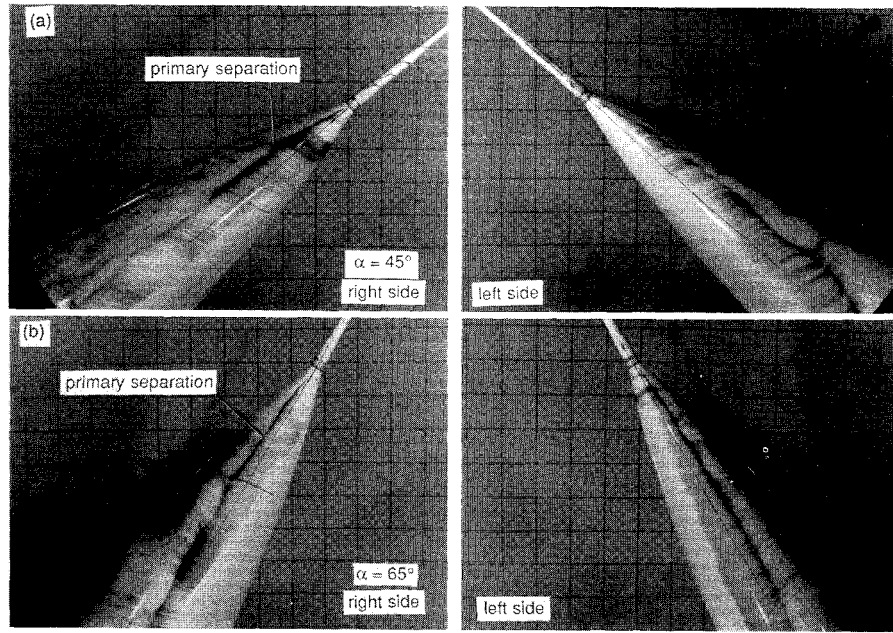


Fig. 2 Surface flow visualization of the F-16 nose-tip model.

angles of attack, evidence of vortex shedding from the nose-boom can be seen.

Details of the flow around the nose-boom and the tip of the forebody are revealed by results of the nose-tip model (model 3) in Fig. 1. At intermediate angles of attack, the flow separates to form a steady and symmetric vortex pair off the tip. At  $\alpha = 30$  deg, the vortex pair becomes asymmetric with the right primary vortex situated above the left. At  $\alpha = 35$

deg, shown in Fig. 1a, the nose-boom tip vortices become strongly asymmetric. The flow off the rear portion of the nose boom begins to form another asymmetric pair of vortices. At increasing angles of attack, this rear vortex pair becomes stronger and can interact with the forebody flow on either the left or right side or both. Although the rear vortex pair is undoubtedly influenced strongly by the tip vortices, only the flow off the rear portion of the nose-boom seems to in-

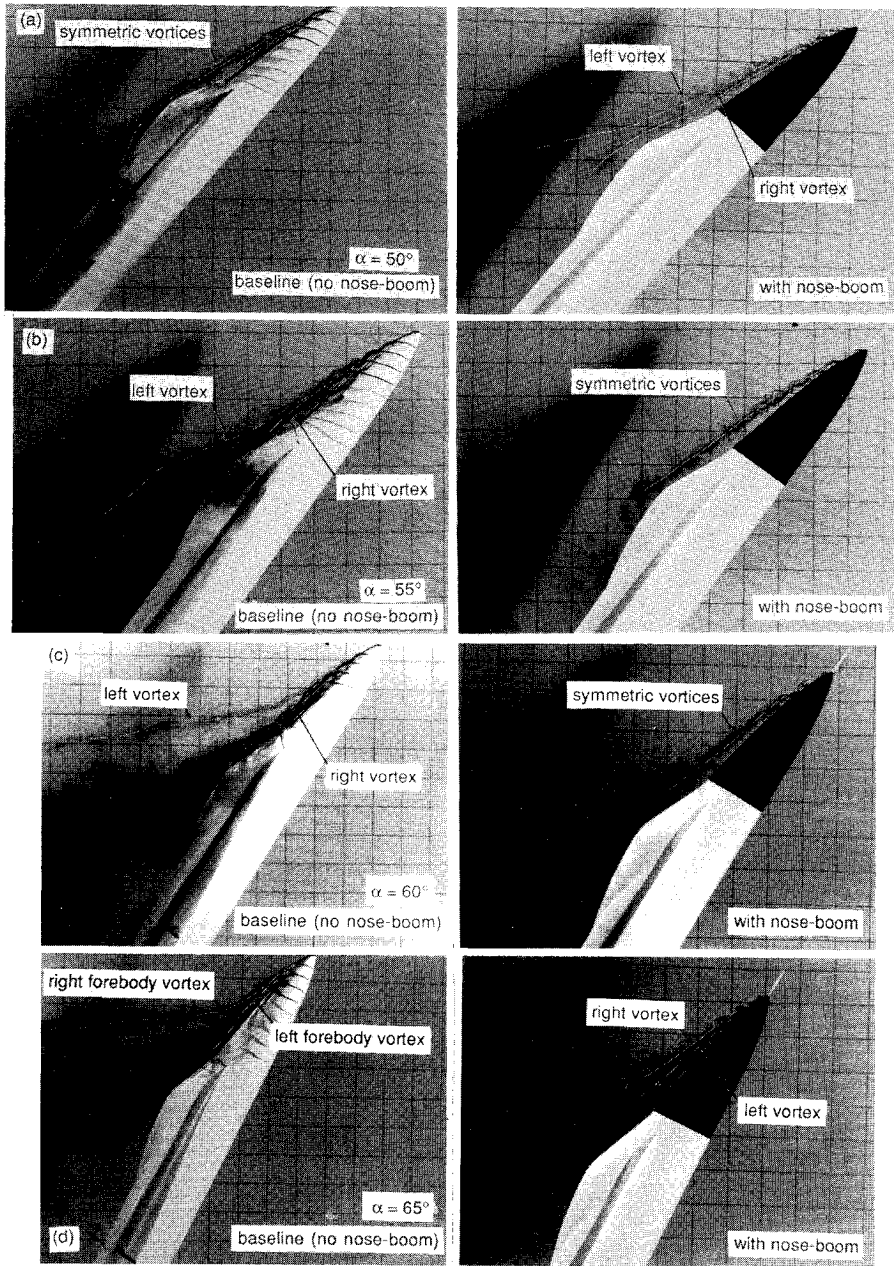


Fig. 3 Effect of a nose-boom on the F-18 forebody flow.

teract directly with the forebody flow. At  $\alpha = 50$  deg, breakdown of the tip vortices of the nose-boom propagates far upstream and the downstream flow becomes more chaotic and seemingly more symmetric. This trend persists at higher angles of attack. At  $\alpha$ 's above about 60 deg, such as the case of  $\alpha = 65$  deg shown in Fig. 1c, unsteady vortex shedding occurs off the rear portion of the nose-boom at a fairly constant frequency.

Thus, the flow off the nose-boom is that of a highly slender, segmented, cylindrical body. When such a body is pitched through angles of attack, it experiences several distinct flow regimes. At moderate angles of attack, the flow separates to form a steady and symmetric vortex pair. At moderate-to-high angles of attack, the vortex pair becomes asymmetric. At high angles of attack, multiple asymmetric vortex pairs form. At very high angles of attack, vortices are shed in the form of a vortex street off the rear portion of the body.

The effect of the nose-boom on the forebody flow is further revealed by the surface flow results of model 3 at increasing angles of attack in Fig. 2. Initially, the primary separation near the tip region is essentially symmetric. The separation becomes asymmetric at  $\alpha$ 's above about 30 deg. The degree

of asymmetry, however, does not follow a specific pattern and can increase or decrease at increasing angle of attack. Maximum asymmetry seems to occur at an  $\alpha$  of about 45 deg, shown in Fig. 2a. Above  $\alpha$  of about 55 deg, such as the case of  $\alpha = 65$  deg shown in Fig. 2b, the separation becomes essentially symmetric again (at least, in a time-average sense).

Naturally, the effect of the nose-boom on the forebody flow is dependent on the specific combination of nose-boom geometry and the baseline (without nose-boom) forebody flow. As mentioned previously, with the differences in Reynolds number and models, results from the three models are not expected to be identical. Nevertheless, the results obtained are very similar both qualitatively and quantitatively. The baseline flow for the F-16 configuration is essentially symmetric through the range of angles of attack tested. The effect of the nose boom is to promote forebody vortex asymmetry over an angle of attack range from about 35–60 deg.

Results of the F/A-18 further demonstrate the relationship between the baseline flow and the effect of the nose-boom. The baseline forebody flow of the F/A-18 model is significantly different from those of the F-16 models. As reported in Ref. 5, from  $\alpha = 15$ –55 deg, the flow is visibly symmetric.

From  $\alpha \approx 55$ –60 deg, the forebody vortices are asymmetric and stable with the left vortex assuming a high position regardless of the history of sideslip. At  $\alpha$ 's among 60 and 65 deg, the flow becomes nearly "bistable." The steady vertical flow tends to assume one of two mirror-image asymmetric flow patterns at a given combination of  $\alpha$  and  $\beta$ , depending on the sideslip history and imposed transient disturbances.<sup>5</sup> The effect of a nose-boom on the baseline F/A-18 flow is illustrated by the examples in Fig. 3. At  $\alpha = 50$  deg, shown in Fig. 3a, the nose-boom causes the forebody vortices to become asymmetric. At  $\alpha = 55$  and 60 deg, shown in Figs. 3b and 3c, respectively, the natural asymmetry is essentially eliminated. At  $\alpha = 65$  deg, shown in Fig. 3d, the asymmetry is reduced but not eliminated.

Therefore, at moderate-to-high angles of attack where the vortex pattern over the nose-boom becomes asymmetric, the wake of a nose-boom seemingly overrides other small naturally present perturbations on the forebody. This can lead either to an increase or a decrease in the natural zero-sideslip forebody vortex asymmetry, depending on the state of the baseline flow. At very high angles of attack where unsteady vortex shedding occurs off the nose boom, the nose-boom wake flow is symmetric on the time-average basis. Evidently, because the shedding frequency of the nose-boom vortices is high compared to the response of the forebody vortex system to imposed disturbances, no significant oscillation of the forebody vortex flow can be observed. The forebody vortex flow is, therefore, essentially symmetric and steady. The main effect of the nose-boom at very high angles of attack would seem to be to reduce forebody vortex asymmetry regardless of the state of the baseline flow.

#### IV. Conclusions

The effect of a nose-boom on forebody vortex flows has been studied in a water tunnel using several different model

configurations. The wake flow of a nose-boom was observed to be similar to that of highly slender cylindrical bodies. The wake consists of symmetric vortices at moderate angles of attack, asymmetric vortices at high angles of attack, and unsteady vortex shedding at very high angles of attack. The influences of these nose-boom-induced vortex-flows are typically strong compared to other natural sources of forebody vortex asymmetry that may be present. The nose-boom, therefore, has a dominating effect on the forebody vortex asymmetry in most situations. At moderate-to-high angles of attack, the net effect can be a reduction or increase in the zero-sideslip forebody vortex asymmetry, depending on the degree of symmetry of the baseline forebody flow without the nose-boom. At very high angles of attack, the typically high vortex-shedding frequency and the comparatively slow response of the forebody vortices to imposed disturbances result in the elimination or reduction of forebody vortex asymmetry.

#### References

- Erickson, G. E., Hall, R. M., Banks, D. W., Del Frate, J. H., Schreiner, J. A., Hanley, R. J., and Pulley, C. M., "Experimental Investigation of the F/A-18 Vortex Flows at Subsonic Through Transonic Speeds," AIAA Paper 89-2222, 1989.
- Hall, R. M., Erickson, G. E., Straka, W. A., Peters, S. E., Maines, B. H., Fox, M. C., Hames, J. E., and LeMay, S. P., "Impact of Nose-Probe Chines on the Vortex Flows about the F-16C," AIAA Paper 90-0386, 1990.
- Keener, E. R., Chapman, G. T., Cohen, L., and Taleghani, J., "Side Forces on a Tangent Ogive Forebody with a Fineness Ratio of 3.5 at High Angles of Attack and Mach Numbers from 0.1 to 0.7," NASA TM X-3437, Feb. 1977.
- Modi, V. J., Ries, T., Kwan, A., and Leung, E., "Aerodynamics of Pointed Forebodies at High Angles of Attack," *Journal of Aircraft*, Vol. 21, No. 6, pp. 428–432.
- Ng, T. T., and Malcolm, G. N., "Aerodynamic Control Using Forebody Blowing and Suction," AIAA Paper 91-0619, 1991.

## Technical Comments

### Comment on "NASA Investigation of a Claimed 'Overlap' Between Two Gust Response Analysis Methods"

Bernard Etkin\*  
*University of Toronto, Toronto,  
 Ontario M2N 6B6, Canada*

THE subject paper<sup>1</sup> provides an interesting and timely comparison of the statistical discrete gust (SDG) and power spectral density (PSD) methods of calculating gust response of aerospace vehicles. Discrete gust methods have a long and honorable history. They have served aviation well for more than half a century,<sup>2</sup> both because of their simplicity, and because they do, indeed, model real events in the atmosphere to a degree that has engineering utility.

Received Oct. 15, 1990; revision received Jan. 13, 1991; accepted for publication Feb. 15, 1991. Copyright © 1991 by the American Institute of Aeronautics and Astronautics, Inc. All rights reserved.

\*University Professor Emeritus, Institute of Aerospace Studies, Fellow AIAA.

The use of a superposition of discrete gusts to model continuous atmospheric turbulence is, however, a quite different matter. The comment attributed in the paper to J. G. Jones "... the former is essentially simply an approximate representation of the latter" is a fair assessment. The paper bears out this assertion in that the claimed equivalence is shown to exist approximately for a special case—that is, input of only vertical gusts to a linear system. One must, however, ask the question, "Why use an approximation when the real thing is available?" Clearly, not to save computing time. The paper shows that the computational cost of the SDG method is more than twenty times that of the PSD method. The reason given in the paper for using SDG is that it provides simultaneous values of many responses (loads) from which practical test loads can be found. This judgment about the PSD method (more properly, conventional random process analysis) is not strictly true. Within the commonly used assumptions of linear systems and Gaussian turbulence, one can, in fact, very easily determine sets of simultaneous loads that exist at any chosen probability level. This is demonstrated below. Thus, this feature of the SDG method is not its main advantage over PSD. The advantage it does have, one that may even be worth the penalty in computing cost, is that it can use non-Gaussian turbulence inputs, because it is well known that atmospheric turbulence has this characteristic. At the same time, certain deficiencies of SDG should be noted. As described, for example in Ref. 3, it makes no provision for variation of vertical